# $c \neq 35H$: A New Model Relating Hemoglobin, Hematocrit, and Optical Density

Katherine Paseman
Bioengineering and Physics
July 2014

## 1 Personal

When I was in the third grade, ten years ago, my mother constantly felt dizzy and tired. She finally sought medical attention and her blood was drawn for testing, but it wasn't until a week later that she was told that her hemoglobin levels were so low that she had to go to the hospital immediately. After a stressful series of months following some procedures, including many more blood draws from my anemic mother, she recovered and was able to return to her normal activities.

The stress involved in my mother's experience began my family's personal crusade to create non-invasive, instant blood analysis. After my sister's research regarding the use of fluorescence to determine iron deficiency, I became fascinated with the other optical properties of blood we could leverage to conduct a wider range of tests.

I was very fortunate in my research journey in that my math and science curricula at school paralleled the knowledge I needed to complete my project. Just as I had learned the meaning of e and log in Pre-Calculus, I began exploring the Beer-Lambert law, a simple exponential function describing how light permeates any material, which I applied to blood. The summer after I'd learned the wave-particle duality of light in AP Physics B, I investigated how light scatters when it encounters a surface in a liquid, for example, a red blood cell suspended in plasma. By the time I was learning multi-variable calculus, I was using six dimensional modeling to succinctly illustrate the many factors which contribute to a person's hemoglobin and hematocrit levels.

While I was blessed with an understanding of the math and science concepts my project required, I was not nearly as lucky when it came to research resources. My research path strays from convention in that by the time my paper was completed, I had collected no data. Testing theories regarding ways to improve medical devices is tedious, requiring a tremendous amount of time, money, energy, and generally support from an academic institution in the form of IRB approval. In spite of my effort, I was unable to generate such support. I made up for this lack of academic interest by creating a solid foundation for my theories and representing my findings in compelling

graphs and geometric models. While not nearly as concrete as working with real data from real patients, the theoretical data used in my paper was sufficient to convincingly convey my findings.

This research journey has taught me so many different lessons, but there are two I consider most important. First, I learned the value of being inquisitive over lunch with my mentor and father. While outlining the layout of my paper and happily munching away on ribs, the figures and numbers swirled in my head, and I realized I was getting all of the different parameters we were keeping track of (SpO2, Hgb, Hct, etc.) confused. I remember asking "Wait, in Figure 11, is the percentSat 100% or 0%?" to which my father replied "That is the right question to be asking." In that moment, we realized that the phenomena we were trying to describe needed to be represented in six dimensions, not just three. This key finding is reported in the final section of my paper.

Second, I learned that the STEM fields actually allow for academic flexibility. My peers have informed me that the humanities are ever popular because "there's more than one right answer," so you can never be wrong. By contrast, in math and science classes, there's always a correct answer and, more often than not, an incorrect answer. In learning about methods of non-invasive blood analysis, I've learned that the room for creativity in science is not in the answer itself , but in the method of finding that answer. Approaching the same question from different angles to find new paths to higher levels of knowledge is exactly what research is about. I believe it is this kind of mental gymnastics that will keep me hooked on STEM for the rest of my life.

## 2 Introduction

We are building a Hemometer, a low cost device which uses light instead of needles to measure two components of a blood panel: Hematocrit fraction (Hct) and Hemoglobin concentration (Hgb). Such a device has many uses: home health monitoring, blood bank pre-screening, etc., but our primary focus is to develop a device which can detect low hemoglobin levels in expectant mothers.

Measuring Hemoglobin by observing how blood transmits light is a well developed idea. The 'Hemoglobin Color Scale' (HCS) [5], which consists of putting blood on paper and comparing it to a color card, is a recent effort which illustrates the difficulties inherent in a colorimetric approach. Results differed substantially between lab and field testing [6]. HCS's inventors listed what they viewed as the key issues in moving HCS from the lab to the field [7].

1. Inadequate or excessive blood
2. Reading the results too soon or too late (beyond the limit of two minutes)
3. Poor lighting
4. Holding the scale at the wrong angle

According to HCS's inventors, "when the tests were repeated under supervision and these faults were avoided: 95% of readings were within $1\frac{g}{dl}$ of the reference measurements, and 97% within $1.5\frac{g}{dl}$ Anaemia screening showed 96% sensitivity and 86% specificity. Clinical judgement of pallor was frequently wrong, whereas the scale gave the correct diagnosis in more than 97% of cases."

When we started our research, this gave us a great deal of hope, since we believed that issues 1 and 2 arose because HCS was invasive and that issues 3 and 4 arose because HCS was manual. As such, we felt that we could address these issues by extending existing non-invasive, automatic, colorimetric approaches. Though these methods introduce issues of their own, we believe that many of these challenges can be overcome by creating a more comprehensive model of blood. In this paper, we develop the mathematical model required to make our Hemometer work by reviewing several existing representations of how raw blood interacts with light, and extending one of them to develop a model based on intuitions from 3D Geometry.

# 3 Prior Work

## 3.1 Pulse Oximetery

There are many mathematical models of how blood interacts with light [8]. One of the oldest is to simply assume that blood absorbs light and so O.D.tot consists of one term: O.D.absorption. O.D.absorption is governed by the Beer-Lambert law which tells us that light intensity through a homogeneous medium drops exponentially both with distance and with concentration of absorbers. By way of example, suppose a red LED is shining through a vial filled with red dye. The Beer Lambert law tells us that if the dye concentration triples, the intensity will drop by a factor of 8. Similarly if the vial diameter is tripled, the intensity will also drop by a factor of 8. This is expressed by:

$$O.D.tot = ln\left(\frac{I_o}{I}\right) = -ln\left(\frac{I}{I_o}\right) = O.D.Absorption = \epsilon cD \tag{1}$$

where

- $O.D.tot$ is Total Optical Density
- $I_o$ is the incident light intensity (light entering the sample)
- $I$ is the transmitted light intensity (light exiting the sample)
- $\epsilon$ is the absorption coefficient and is dependent on wavelength $\lambda$
- $c$ is the concentration of the absorbent
- D is the optical path length of the sample

Though Beer-Lambert rather crudely models blood as a red dye (with no light scattering cell surfaces), Pulse Oximetry practitioners are able to use it to non-invasively determine Blood's SpO2 concentration with just two additional equations. First, they equate the pulsatile light intensity (systolicIntensity/diastolicIntensity) transmitted through the finger to I/Io, so

$$ln(\frac{I}{I_o}) = ln(\frac{systolicIntensity}{diastolicIndentisty}) = -ln(\frac{I_o}{I}) = -O.D.tot(\lambda, D, c) \tag{2}$$

Second, they note that the ratio of two optical densities at two different wavelengths (typically red (e.g. 660 nm) and infrared (e.g. 940 nm) creates a number that is both independent of 'D' and proportional to SpO2 (Dissolved Blood Oxygen). This second equation is called 'Ratio of Ratios." Again, note that 'R' is independent of 'D'.

$$R(c) = \frac{O.D.tot(Red, D, c)}{O.D.tot(Infrared, D, c)} \tag{3}$$

### 3.2 Twersky [4]

Though modeling blood as a red dye is good enough for Pulse Oximetry's SpO2 concentration measurements, it does not model Hemoglobin concentration or Hematocrit fraction well. More accurate models require representing blood as a solution which absorbs and scatters light. [9]

Steinke compared O.D.tot measurements made through whole blood in a lab to three different mathematical models. The first, Twersky [4], was based on electro-magnetic wave theory. The second, Zdrojkowski [10], was based on photon diffusion theory. The third, Loewinger [11], used a "semi-empirical" theory. Twersky's model matched experimental data best. This was corroborated later by De Kock and Tarassenko[12].

Twersky's basic model extends the absorption model described above by adding a scattering term.

$$O.D.tot = O.D.absorption - log_{10}(celltocellscattering + incoherentscattering) \tag{4}$$

where

- $O.D.absorption = \epsilon cD$
- $celltocellscattering = 10^{-aDH(1-H)}$
- $incoherentscattering = q(1 - 10^{-aDH(1-H)})$

Substituting gives

$$O.D.tot = \epsilon cD - log_{10}[10^{-aDH(1-H)} + q(1 - 10^{-aDH(1-H)})] \tag{5}$$

where

- $a$ = a constant dependent upon particle size, $n_{Hb}$ (hemoglobin index of refraction), $n_{plasma}$ (plasma index of refraction), and $\lambda$.
- $H$=fractional Hematocrit
- $q$ = a constant dependent upon particle size, $n_{Hb}$, $n_{plasma}$, $\lambda$, and the photodetector aperture angle.

### 3.3 Steinke[3]

Steinke introduced a 'backscattering' version of this equation:

$$O.D.tot = mH - log_{10}[(1-q)10^{-\beta} + q10^{-\delta}] \tag{6}$$

where

- $\beta = aDH(1-H)$
- $\delta = 2q'maDH\frac{1-H}{2m+aD(1-H)}$
- $q'$ = is a parameter of the particular design which couples absorbance and scattering and depends on $\lambda$ and the spectral properties of the LED. It varies between 0 and 1.
- mH *"replaces $\epsilon cD$"*(our emphasis) . In a Table II footnote, Steinke also notes that he assumes $H = cHb/(\frac{35g}{100ml})$.

  The $H = cHb/(\frac{35g}{100ml})$ (our emphasis) constraint was maintained by Steinke in his lab work and allowed him to report O.D.tot a function of a single variable.

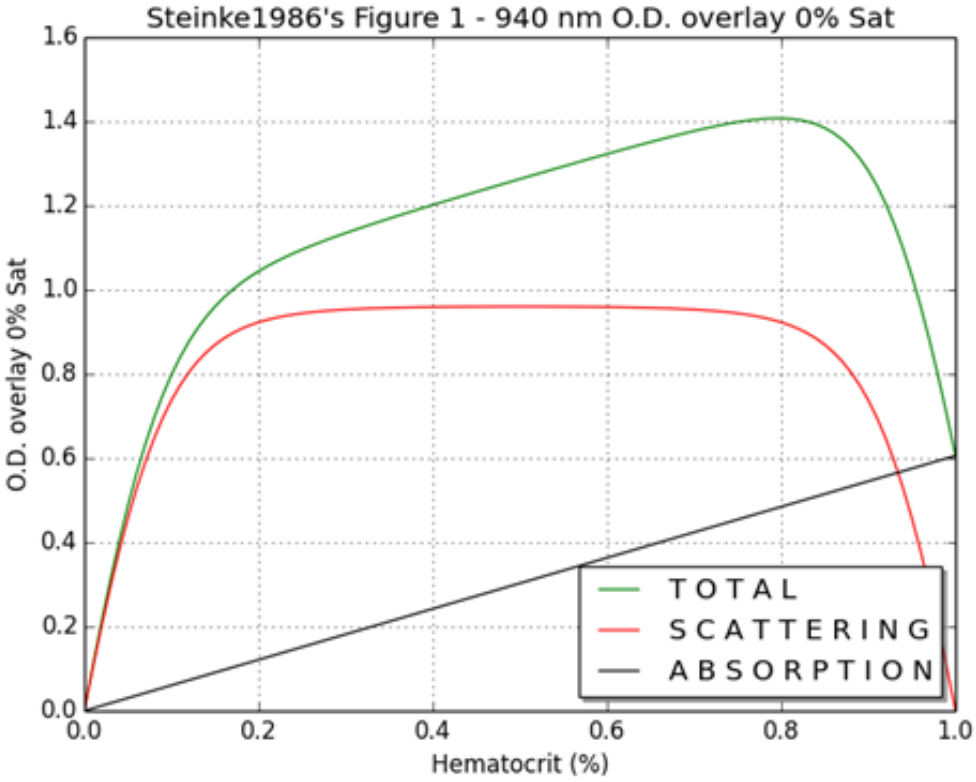


Figure 1: Steinke's equations are reproduced for 940 nm light through a 1.61 mm cuvette filled with de-oxygenated dog's blood. The linear absorption term is in black. The scattering term is in red and the sum of the two equations, O.D.tot, is in green. This figure was generated by a Python program using Steinke's models and extinction coefficients from Prahl [13].

### 3.3.1 Jello Balls as a Model for Scattering

As an aside, note that the scattering portion is symmetric. A thought experiment using a beaker of water (modeling plasma) and a handful of small red Jello balls (modeling blood cells) can help us see why. If we shine a light through a beaker containing just water, we get a Beer-Lambert's law response. Suppose we add one small red Jello ball. Some of the light will scatter away, decreasing output intensity, and thus increasing O.D.tot. As we add more balls, eventually we hit a point where the beaker is full, composed of half Jello and half water. The only way we can add more balls to a full beaker is if we squeeze them in, causing the water in the beaker to spill over the top. This has two effects. First, it reduces the water volume between the balls; second, it reduces the total surface area that refracts light. As a result, O.D.tot starts to decrease. On this side of the curve, the model is not how light bounces off the surface of the Jello balls in water, but how light bounces off the surface of water balls in Jello. Eventually we have 100% Jello and Beer-Lambert behavior again. This thought experiment was confirmed by Loewinger who noted that at H=1, packed cells obeyed Beer's law.

### 3.4 Jeon [2]

Jeon and Yoon combined Steinke's invasive blood measurement work with a non-invasive pulse oximeter-like probe and noted that the scattering portion of Twersky's model looks like a parabola if D is small enough. By using a parabolic approximation and incorporating Steinke's $c = 35H$ assumption, both Jeon and Yoon created the closed form solution for R shown below.

$$R(\lambda_1, \lambda_2) = \frac{\frac{AC(\lambda_1)}{DC(\lambda_1)}}{\frac{AC(\lambda_2)}{DC(\lambda_2)}} = \frac{35\epsilon(\lambda_1) + k(\lambda_1)a(\lambda_1)H(1-H)}{35\epsilon(\lambda_2) + k(\lambda_2)a(\lambda_2)H(1-H)} \tag{7}$$

where

- $AC(\lambda)$ = pulsatile component of the waveform at wavelength $\lambda$
- $DC(\lambda)$ = nonpulsatile component of the waveform at wavelength $\lambda$
- $\lambda$ = wavelength - 569, 660, 805, 904, and 975 were used
- $\epsilon$ = extinction coefficient
- k = value depends on the optical design of the system
- a = shape function of red blood cells
- H= hematocrit

As Jeon notes and as the figures generated by our Python model (below) show, the parabolic approximation works best for small $D$ and worsens for larger $D$. This brings forth a critical question: How large should we estimate $D$ to be? Jeon estimates it to be smaller than 0.05 mm.

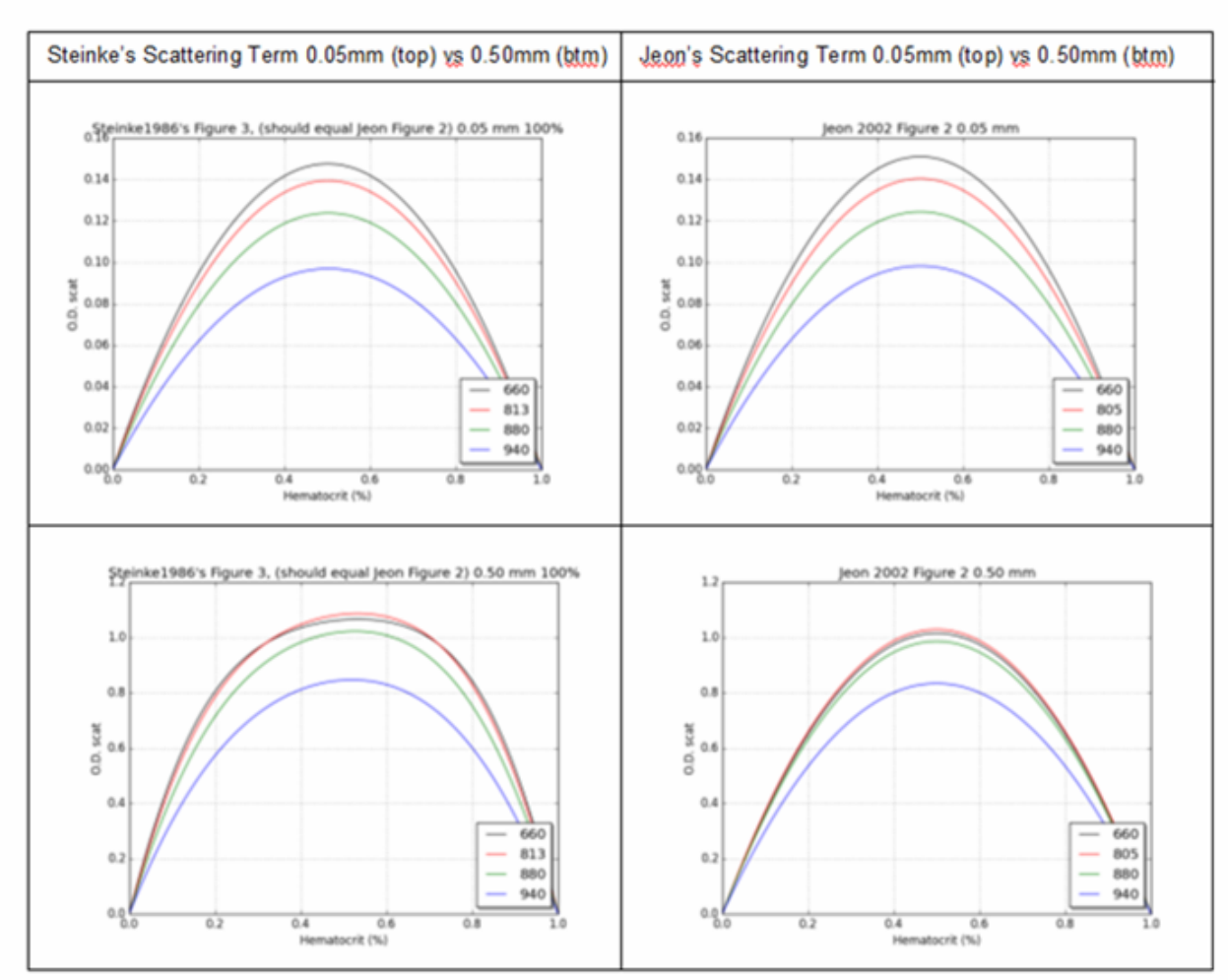


Figure 2: As Jeon notes, the parabolic approximation works best for small D and worsens for larger $D$.

## 4 c $\neq$ 35H

Now, though Steinke's lab work set $c = 35H$, and Jeon carried this forward as a constraint in her work, Hemoglobin concentration is not really equal to 35 times Hematocrit (that's why we have Blood Panels). So suppose we abandon the $c = 35H$ simplification and just treated Hgb and Hct as two independent variables? After all, as Steinke notes: "The interesting feature of [equation 5], as mentioned by Lipowsky [14], is that it essentially resolves the total O.D. into two distinct parts. The first term $\epsilon cD$ is a Beer's Law expression for the absorption by the hemoglobin in the cells, and the second term describes the attenuation of light due to scattering. Hence, according to this equation, the absorption and scattering of light can be treated as two independent processes."

In that case, we can move from an algebraic view of the data to a 3D geometric view by just "folding out" either Steinke's Figure I or any of Jeon's diagrams.

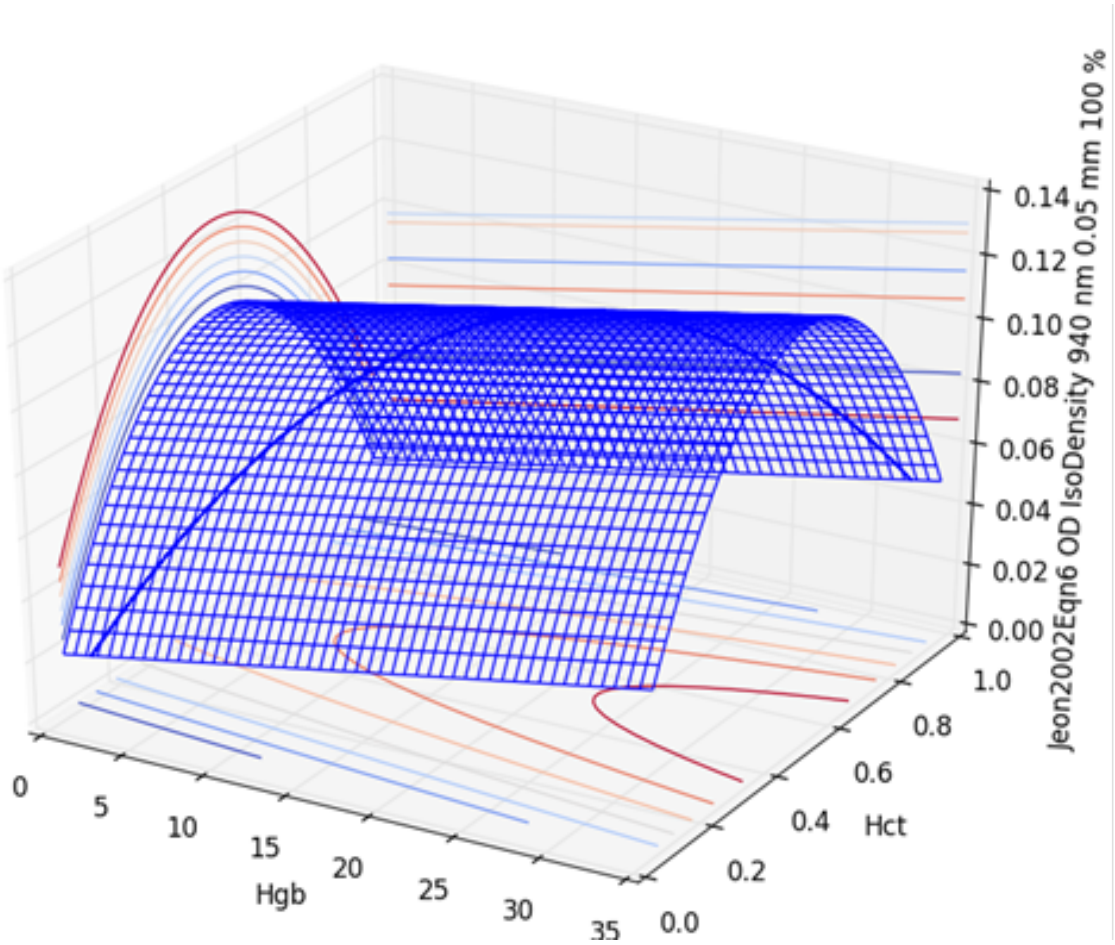


Figure 3: Here, Hct and Hgb are on the x and y axes respectively and O.D.tot is on the z axis. The thick blue line on the figure's surface shows where $Hgb = 35 \times Hct$. Data comes from the parameters reported in Steinke [3] and Jeon [2].

At this point, we must differentiate the three projections onto each of the three planes.

- The first is the projection onto the surface of the Hgb/O.D.tot plane at constant Hct. This is just the straight line Beer-Lambert absorption term.
- The second is the projection of the surface onto the Hct/O.D.tot plane at constant Hgb. This is just the parabolic scattering term.
- The third is the projection of the surface onto the Hgb/Hct plane at constant O.D.tot. Though parabolic, it is not the same as the parabolic Hct/O.D.tot projection. It is this last class of projections that we examine in the next section.

# 5 Geometric Method to Determine Hgb and Hct from two O.D.tot measurements and D

We can use $D$ and these surfaces' projections on the Hgb/Hct plane to determine Hgb and Hct using just two O.D.tot measurements without the $c = 35H$ simplification. We demonstrate this visually below using Steinke's backscattering formula plus the Standard Beer-Lambert absorption formula (without the $c = 35H$ simplification).

$$O.D.tot = \epsilon cD - log[(1-q)10^{-\beta} + q10^{-\delta}] \tag{8}$$

where

- $\epsilon$ = absorption coefficient
- $c$ = concentration of the absorbent
- $D$ = optical path length of the sample
- $q$ = a constant dependent upon particle size, $n_{Hb}$ (hemoglobin index of refraction), $n_{plasma}$ (plasma index of refraction), $\lambda$ and the photodetector aperture angle.
- $\beta = aDH(1-H)$
- $\delta = 2q'maD\frac{H(1-H)}{2m+aD(1-H)}$
- $q'$ = a parameter of the particular design which couples absorbance and scattering and depends on $\lambda$ and the spectral properties of the LED. It varies between 0 and 1.
- $H$ = fractional Hematocrit

First, we create two 3d surfaces (Figure 4) by plotting equation 8 with Hct and Hgb on the independent axes (x, y) and O.D.tot on the dependent (z) axis for wavelengths $\lambda_1$ (880 nm) and $\lambda_2$ (660 nm) with D = 0.05 mm and SpO2 = 100%. Note that every interrogation wavelength ($\lambda$) will have its own associated 3d surface.

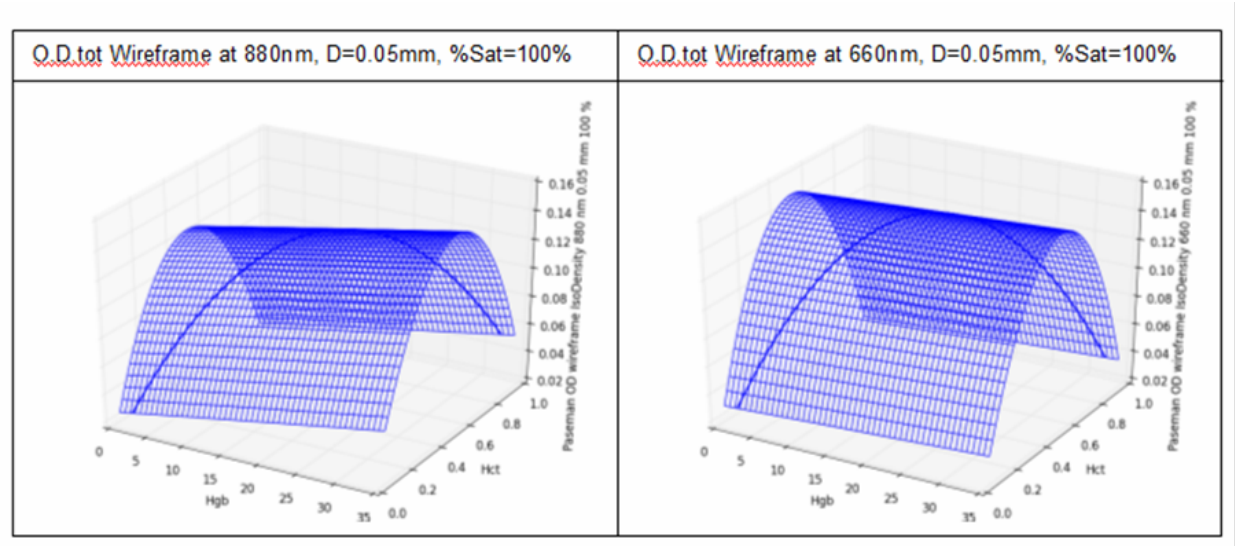


Figure 4: O.D.tot at 880 and 660 nm, D = 0.05 mm, SpO2 = 100%

Second, we note that "IsoDensity" curves are created when each 3D surface is cut with planes at specific O.D.tots.

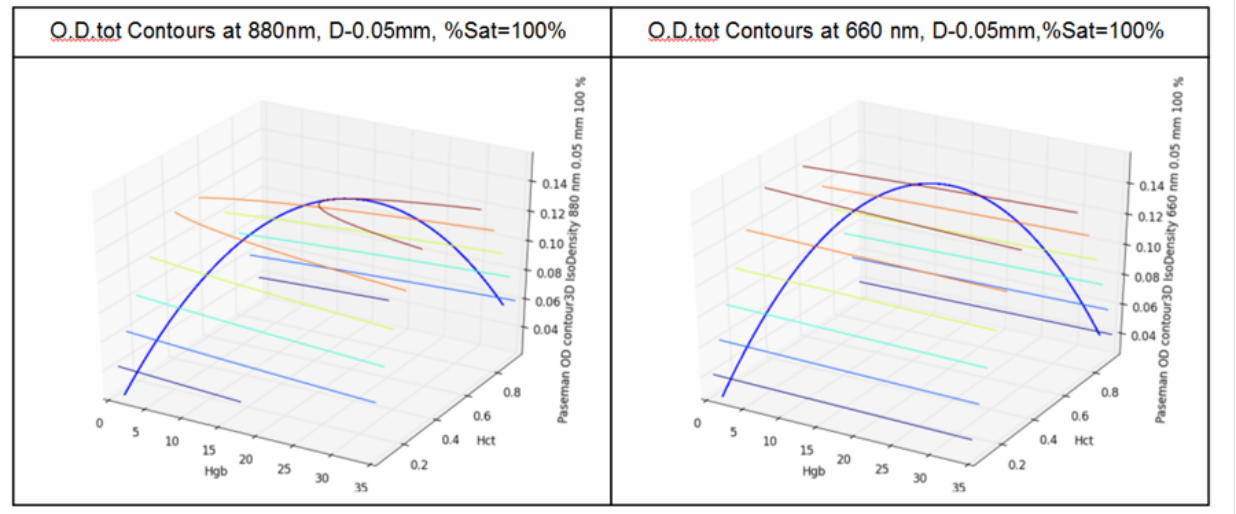


Figure 5: Each curve describes all valid Hgb, Hct values associated with given O.D.tot at a specific $\lambda$. As in Figure 4, the $c = 35H$ line is in blue.

Third, we project a particular (measured) O.D.tot 1 to form curve 1 from the surface associated with $\lambda_1$ and a particular (measured) O.D.tot 2 to form curve 2 from the surface associated with $\lambda_2$ into the Hgb/Hct plane. Several such projections are shown for each $\lambda$ in Figure 6. Note however, that when there is a single measurement on a single subject, only one isodensity curve is generated per $\lambda$ per subject. For the sake of this example, we will assume that the 880 nm orange isodensity curve and the 660 nm red isodensity curve are generated.

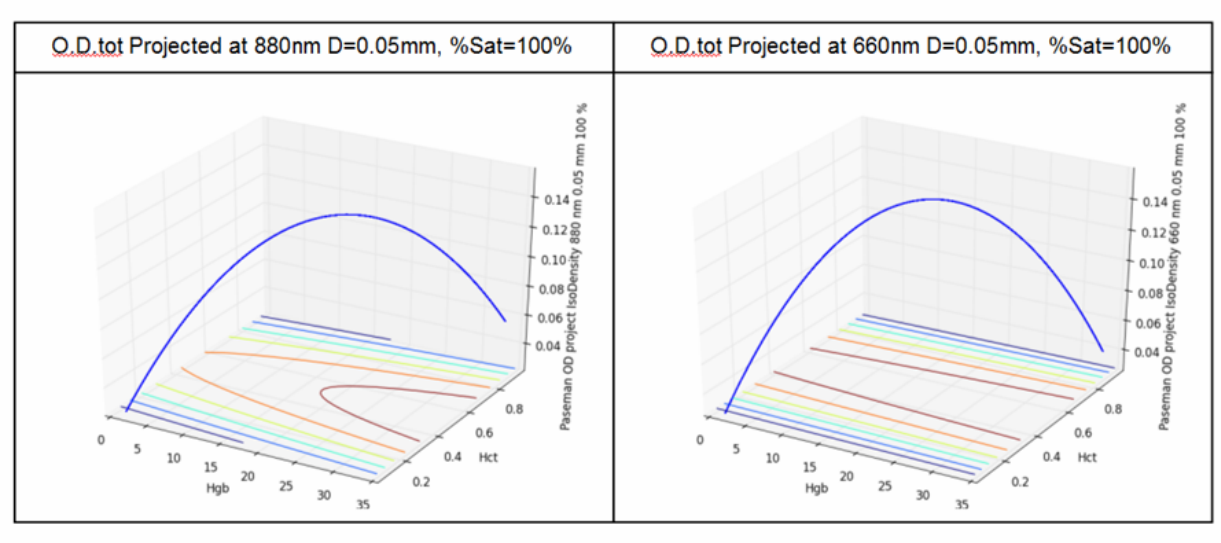


Figure 6: As D is increased, the isodensity curves here become wider just as shown above in 3.4

Finally, we overlay the planes on one another. Due to the dual nature of scattering discussed in Section 3.3.1, there are potentially two points of intersection. The spots where contours intersect are the Hgb, Hct values that satisfy both curves. Again, for the sake of this example, this is where the orange and red isodensity curves intersect, at about Hct $= 0.4, 0.6$ and Hgb $= 4\ \frac{\text{g}}{\text{dl}}$. Note that neither dual number predicted by the constraint $0.4 \times 35 = 14.8\ \frac{\text{g}}{\text{dl}}$ or $0.6 \times 35 = 21\ \frac{\text{g}}{\text{dl}}$ is the same as the number at the these intersections. Although more analysis needs to be done, we suspect that the correct Hct value to pick is the one closest to the $c = 35H$ line. Critically, Hgb aliases to the same value for both points.

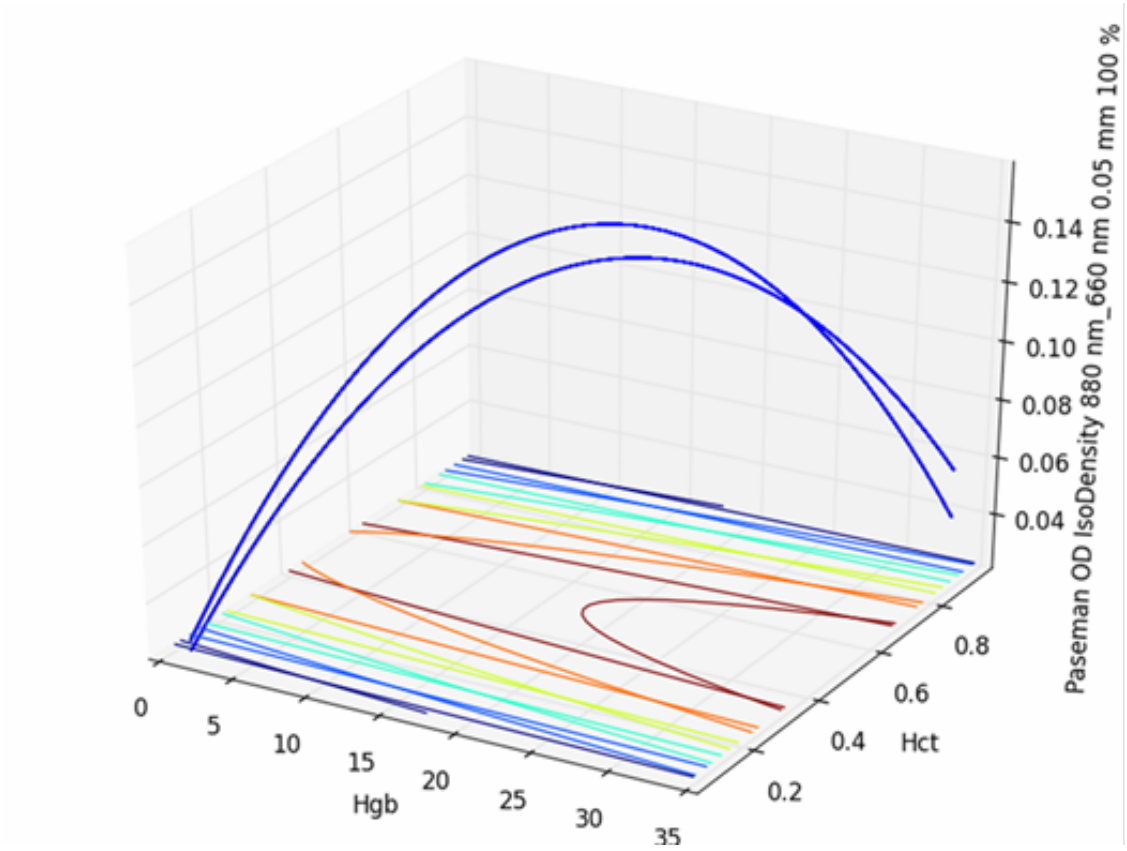


Figure 7: The spots where contours intersect are the Hgb, Hct values that satisfy both curves.

# 6 Analytical Method to Determine Hgb and Hct from two O.D.tot measurements and 'D'

If we use Jeon's parabolic approximation for the scattering term at small D, but keep the Beer-Lambert absorption term:

$$O.D.tot(\lambda) = \epsilon(\lambda)cD + H(1-H)k(\lambda)a(\lambda)D \tag{9}$$

We can create a closed form solution for Hgb and Hct in terms of two O.D.tot measurements and D by first re-casting the equation in standard quadratic form:

$$c = \frac{H(H-1)k(\lambda)a(\lambda)D}{\epsilon(\lambda)D} + \frac{O.D.tot(\lambda)}{\epsilon(\lambda)D} \tag{10}$$

Then dividing out D in the first term:

$$c = \frac{H(H-1)k(\lambda)a(\lambda)}{\epsilon(\lambda)} + \frac{O.D.tot(\lambda)}{\epsilon(\lambda)D} \tag{11}$$

and recognizing that where the parabolas intersect for two different wavelengths, the values of c are equal:

$$H(H-1)\frac{k(\lambda_1)a(\lambda_1)}{\epsilon(\lambda_1)} + \frac{O.D.tot(\lambda_1)}{\epsilon(\lambda_1)D} = H(H-1)\frac{k(\lambda_2)a(\lambda_2)}{\epsilon(\lambda_2)} + \frac{O.D.tot(\lambda_2)}{\epsilon(\lambda_2)D} \tag{12}$$

We can solve this quadratic equation first by regrouping

$$0 = \left(\frac{k(\lambda_1)a(\lambda_1)}{\epsilon(\lambda_1)} - \frac{k(\lambda_2)a(\lambda_2)}{\epsilon(\lambda_2)}\right)H(H-1) + \frac{O.D.tot(\lambda_1)}{\epsilon(\lambda_1)D} - \frac{O.D.tot(\lambda_2)}{\epsilon(\lambda_2)D} \tag{13}$$

and note that the roots of $y = ax^2 + bx + c$ are $x = \frac{-b \pm \sqrt{b^2 4ac}}{2a}$, but when $-b = a$

$$x = \frac{a \pm \sqrt{a^2 - 4ac}}{2a} = \frac{1}{2} \pm \sqrt{\frac{1}{4} - \frac{c}{a}} \tag{14}$$

Giving us the closed form solution

$$H = \frac{1}{2} \pm \sqrt{\frac{1}{4} - \left(\frac{O.D.tot(\lambda_1)}{\epsilon(\lambda_1)KD} - \frac{O.D.tot(\lambda_2)}{\epsilon(\lambda_2)KD}\right)} \tag{15}$$

where

$$K = \frac{k(\lambda_1)a(\lambda_1)}{\epsilon(\lambda_1)} - \frac{k(\lambda_2)a(\lambda_2)}{\epsilon(\lambda_2)} \tag{16}$$

Once we have H, we can obtain c from equation 11.

### 6.1 Elimination of 'D'

If equation 15 could be coaxed into a linear form, we could just take another O.D.tot measurement, and eliminate $D$ in the usual way.
Unfortunately, as Figure 8 shows, members of this class of function do not intersect.

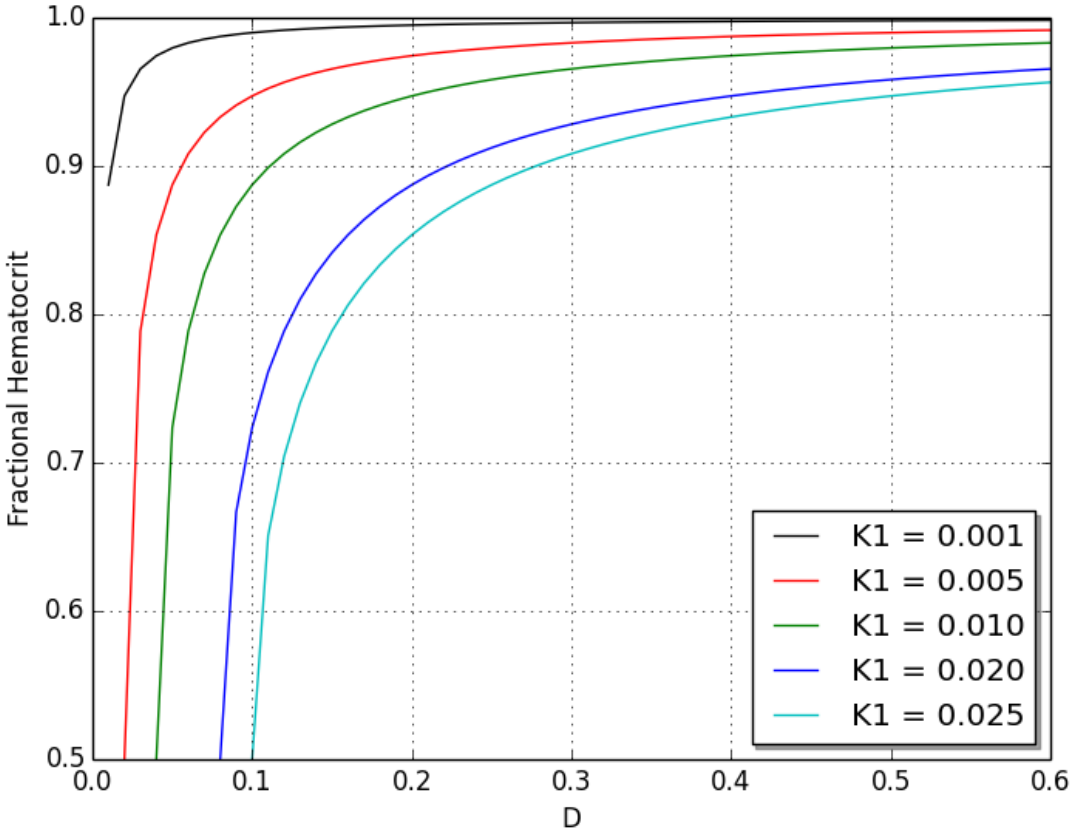


Figure 8: $H = \frac{1}{2} + \sqrt{\frac{1}{4} - \frac{K_1}{D}}$ where $K_1 = \left(\frac{O.D.tot(\lambda_1)}{\epsilon(\lambda_1)K} - \frac{O.D.tot(\lambda_2)}{\epsilon(\lambda_2)K}\right)$

# 7 Method

We created our initial models in Python using the equations and constants reported in Steinke [3], Jeon [2] and Yoon [1]. We validated our models by visually comparing our generated pictures to the ones they reported. We discovered that the extinction coefficients varied significantly between those reported by Steinke and Prahl, so we used those from Prahl. In addition, Jeon did not report data for 569 nm, so we used 805 nm (another isobestic wavelength) which was reported in our analysis. Jeon did not report values for their 'a' parameter, so we deduced them from their reported values of k and D in two steps. First we measured ODmaxes by hand as the maximum values in Jeon [2] which should correspond to 50% Hct. Next, we noted:

$$O.D.scat = kaDH(1 - H) \tag{17}$$

so at 50% Hct,

$$O.D.max = kaD(.5)(1 - .5) \tag{18}$$

so

$$a = 4\frac{O.D.max}{k \times D} \tag{19}$$

Jeon does not say whether equation 18 uses Hb or HbO2 parameters. We assumed HbO2. We then averaged the a's using the ODmaxes from all of Jeon's graphs compared the a's we calculated with those reported by Steinke.

- Jeon a Avg= 13.28, a Deviation = 6.35 percent, Steinke a = 12.92
- Jeon a Avg= 12.23, a Deviation = 4.57 percent, Steinke1986 a = 12.08
- Jeon a Avg= 10.81, a Deviation = 3.82 percent, Steinke1986 a = 10.71
- Jeon a Avg= 8.61, a Deviation = 0.91 percent, Steinke1986 a = 8.46

The primary purpose of this exercise and of reproducing the prior work's Figures (e.g. sections 3.3 and 3.4) was to verify that Steinke and Jeon's models had been copied faithfully into the Python program.

# 8 Results and Analysis

## 8.1 DataCube

Modeling O.D.tot as a function of 5 dependent variables

$$O.D.tot(Hgb, Hct, \lambda, D, percentSat)^1 \tag{20}$$

enabled us to use a datacube-style data analysis approach to gain geometric insights from various projections of O.D.tot's 6-dimensional surface. In particular:

- Same interface for all models: As shown, we parameterized $O.D.tot(Hgb, Hct, \lambda, D, percentSat)$ with Steinke's model, Jeon's model and various combinations of the two. In fact, Hgb and Hct do not even need to be independent. It is sufficient that O.D.tot is simply a function of its passed parameters.

- Functional Model Assumption: Since O.D.tot is modeled as a function, setting some parameters constant (e.g. using a particular $\lambda$) will not cause contours to overlap. Among other things, this means that we believe we have all parameters necessary to characterize the problem.

- Effect of $\lambda$ and $D$ on the "Two O.D.tot and D" method: If the two $\lambda$s are close together, we can expect greater measurement error. As $D$ is increased, the Isodensity curves become wider just as shown in the "Jeon" section.

- "Ratio of Ratios:" for Hgb and Hct at 660/940 nm - Jeon estimates arterial dilation during a heartbeat to be less than several percent of 0.3-1.5 mm or less than 0.05 mm. The change at 50% Hct (the peak of the parabola) from D=.05 to D=.10 is about 1 $\frac{gm}{dl}$ or about 6%. The error is less on either side of 50% Hct. This should bound worst case error.

- "Ratio of Ratios:" for Hgb and Hct at isobestic points: Yoon and Jeon use isosbestic wavelength in 4 out of 5 of the ratios (R569/660, R569/805, R569/940, R569/975, R805/940) to predict Hgb. Although they do not report data for their key isosbestic wavelength, 569 nm, they do report data for another isosbestic wavelenght, 805 nm. Surfaces of ratios of R660/805, R880/805, and R940/805 and also $D$ dependent and the variations at 50% are about the same as R660/940.

[1] In this model, we treat Hgb (Hemoglobin concentration) as one independent variable and percentSat (the degree to which the Hemoglobin is saturated with Oxygen) as another. Parameters such as extinction coefficient were treated as functions of these independent variables and we considered two percentSat values: 0% (Hgb) and 100% (HgbO2) in our analysis.

- SpO2 has a dramatic effect on "Ratio of Ratios" analysis - This tells us that whatever model we employ, it probably makes sense to include an oxygen saturation component (or its Pulseoximeter proxy (e.g. R660/940)).
- "Intersection of Ratios" at isosbestic points: We could not use the intersection method to predict Hgb and Hct using ratio of ratios curves, since overlaying them produces concentric curves.

### 8.2 Hemoglobin Color Scale

In the course of this investigation, we have done our best to squeeze dry the data sources available to us. Given the plethora of parameterized models and 3D graphics we have generated and examined, we'd now like to circle back to the hemoglobin color scale (HCS) described in Section 2. We have annotated the "criteria for failure" observations made by its inventors[7] below with our own answers to the question: "Why does HCS work in the lab?"

1. (uniform 'D') Inadequate or excessive blood - Where blood viscosity does not vary much and when a known volume is applied to a card spot of known area and absorbency[2], the sample will have a uniform thickness and (reflected) light will penetrate only so far.
2. (SpO2) Reading the results too soon or too late (beyond the limit of two minutes) - Waiting a prescribed amount of time creates a sample with uniform SpO2.
3. (wavelength) Poor lighting - Looking at blood in white light, the human eye registers no wavelengths above red and blood absorbs all wavelengths below red.
4. Holding the scale at the wrong angle

So, if nothing else, our research has given us a new appreciation of the insights one can gain from smearing blood on cardboard.

## 9 Conclusions

We believe that the exercise of removing the $c = 35H$ constraint was successful. It allowed us to create a new model relating optical density, hemoglobin and hematocrit. In addition, based on the above observations and analysis, we are hopeful that our model $OD(Hgb, Hct, lambda, \Delta D, \%sat)$ embodies at least a subset of the correct parameters.

[2] Absorbency - as in how a paper towel sucks up water

# 10 Bibliography


1. Yoon, G., Lee, J.Y., Jeon, K.J., Park, K.K., & Kim, H.S. (2005). Development of a compact home health monitor for telemedicine. Telemed J E Health, 11(6), 660-667.
2. Jeon, K. J., Kim, S.-J., Park, K. K., Kim, J.-W., & Yoon, G. (2002). Noninvasive total hemoglobin measurement. J Biomed Opt, 7(1), 45-50.
3. Steinke, J. M., & Shepherd, A. P. (1986). Role of light scattering in whole blood oximetry. IEEE Trans Biomed Eng., 33(3), 294-301.
4. Twersky, V. (1970). Absorption and multiple scattering by biological suspensions. Journal of the Optical Society of America, 60(8), 1084-1093.
5. Lewis, S.M., Stott, G.J., & Wynn, K.J. (1998). An inexpensive and reliable new haemoglobin colour scale for assessing anaemia. J Clin Pathol, 51(1), 21-24.
6. Critchley, J., & Bates, I. (2005). Haemoglobin colour scale for anaemia diagnosis where there iis no laboratory: A systematic review. , International Journal of Epidemiology, 34(6), 1425-1434.
7. Ingram, C.F., & Lewis, S.M. (2000). Clinical use of WHO haemoglobin colour scale: Validation and critique. J Clin Pathol, 53(12), 933-937.
8. Ito, Y., Kawaguchi, F., Kohida, H., Negai, K., & Yoshida, M. (1993). U.S. Patent No. US5239185 A. Washington, DC: U.S. Patent and Trademark Office.
9. Webster, J.G. (Ed.). (1997). Medical Physics and Biomedical Engineering: Design of pulse oximeters.
10. Zdrojkowski, R.J., & Pisharoty, N.R. (1970). Optical transmission and reflection by blood. IEEE Trans Biomed Eng, 17(2), 122-128.
11. Loewinger, E., Gordon, A., Weinreb, A., & Gross, J. (1964). Analysis of a micromethod for transmission oximetry of whole blood. Journal of Applied Physiology, 19(6), 1179-1183.
12. de Kook, J.P., & Tarassenko, L. (1993). Pulse oximetry: Theoretical and experimental models. Med Biol Eng Comput., 31(3), 291-300. Method and equipment for measuring absorptance of light scattering materials using plural wavelengths of light
13. Prahl, S. (1998, March 4). Tabulated molar xxtinction coefficient for hemoglobin in water. Retrieved November 10, 2013, from http://omlc.ogi.edu/spectra/hemoglobin/summary.html
14. Lipowsky, H. H., Usami, S., Chien, S., & Pittman, R. N. (1980). Hematocrit determination in small bore tubes from optical density measurements under white light illumination. Microvascular Research, 20, 51-70.
15. Paseman, K. (2013, March). Improving non-invasive blood analysis. Retrieved November 9, 2013, from http://hemometer.tumblr.com